Preprints of the 21st IFAC World Congress (Virtual)
Berlin, Germany, July 12-17, 2020

Energy Management of Heavy-Duty Fuel Cell Electric Vehicles: Model Predictive Control for Fuel Consumption and Lifetime Optimization

Alessandro Ferrara*. Michael Okoli*. Stefan Jakubek*. Christoph Hametner**

**Institute of Mechanics and Mechatronics, TU Wien, Austria (e-mail: alessandro.ferrara@tuwien.ac.at)*
***Christian Doppler Laboratory for Innovative Control and Monitoring of Automotive Powertrain Systems, TU Wien, Austria, (e-mail: christoph.hametner@tuwien.ac.at)*

Abstract: This paper investigates the application of a simple but effective model predictive control concept for the fuel consumption and system lifetime optimization of a heavy-duty fuel cell electric vehicle. Energy management strategies primarily help extend the fuel cell lifetime by limiting shutdowns, transients and high-power operations to avoid detrimental conditions. In this framework, the proposed online control scheme determines a significant reduction of the average fuel cell power change rate and a small fuel consumption increment with respect to the control law that minimizes the fuel consumption, computed offline through the Pontryagin's minimum principle. These results refer to the real-world driving mission of a road freight vehicle, including the elevation gradient of the road, which highly affects the load request in downhill and uphill sections. However, this preliminary study does not include a speed prediction model, but it assumes that the speed is known without uncertainties over a relatively short time horizon.

Keywords: Optimal Control, Online Energy Management, FCEV, MPC, PMP, Fuel Cell Degradation.

1. INTRODUCTION

Zero-emission vehicles such as battery electric vehicles (BEVs) or fuel cell electric vehicles (FCEVs) play a major role in the decarbonization process of the ground transport sector. These vehicles are already available on the market of passenger cars and they have shown promising results in terms of performance, driving comfort and range. Conversely, higher power and range requirements hinder the diffusion of zero-emission heavy-duty vehicles. In this framework fuel cell systems (FCS), which are usually based on proton exchange membrane fuel cells (PEMFCs), seem more appealing than battery systems thanks to their higher energy density, fast refuelling time and modularity, which is useful for different vehicle size configurations. However, the commercialization of heavy-duty FCEVs is limited by their lower durability and reliability compared to conventional vehicles, by higher manufacturing costs and because of the missing hydrogen refuelling infrastructure.

Control strategies are fundamental to suitably operate fuel cell systems and to increase their durability and reliability. In hybrid vehicles, the energy management strategy (EMS) distributes the load request to the power sources and it is usually designed to minimize the fuel consumption. The advantages of using such EMSs are enormous in hybrid electric vehicles (HEVs) because the efficiency of internal combustion engines varies considerably with their rotational speed and torque. But in FCEVs the EMS impacts less significantly on the fuel consumption because the efficiency characteristic of fuel cells is relatively flat over the power range. In this case, the EMS should also focus on extending the lifetime of the fuel cell system and/or of the battery system. The low-level controllers receive as input the power setpoints from the EMS (i.e. the high-level controller). During normal operation, the fuel cell controller must properly act on the reactant supply, and the water and thermal managements to avoid – or limit – the occurrence of detrimental conditions. Dehydration and high temperatures, indeed, can determine an irreversible deterioration of the membrane electrode assembly, even if they occur for limited time. Reactant starvation can cause critical local potentials and accelerate the corrosion of carbon supports, severely affecting the fuel cell lifetime and performance due to the permanent loss of electrochemically active area. During a start-up it is not possible to avoid the localized hydrogen starvation due to the inevitable transition between air-filled and fuel-filled anodes (or vice versa during a shut-down). Nonetheless, localized hydrogen starvation can also be caused by poor water management, poor cell-to-cell fuel distribution, high-power operation and fast up-load transients (Perry 2006, Borup 2007). Clearly, the fuel cell control is a complex task even during its normal operation. Nevertheless, vehicle applications expose fuel cell systems to frequent start-up/shut-down cycles, dynamic loads, idling operation and cold starts, causing reactant starvation and many temperature and relative humidity changes. Thus, the overall fuel cell control is more difficult compared to stationary applications, and the fuel cell lifetime is considerably shorter. Measures of the voltage degradation rate, indeed, show a magnitude of ~1 $\mu V \cdot h^{-1}$ during stationary operation and ~100 $\mu V \cdot h^{-1}$ during dynamic operation (Zhao 2019). These findings indicate that, even if the fuel cell degradation depends on many factors and it requires detailed modelling to be quantified in a meaningful way, the high level controller can still significantly contribute to the degradation mitigation through the stationary operation of the fuel cell system.

The energy management problem has been studied extensively for HEVs over the last decade. More recently, some works examined the energy management problem of FCEVs focusing on the simultaneous optimization of fuel consumption and system lifetime. In (Xu 2014) a multi-mode real-time EMS of a plug-in FCEV bus is proposed. Three different control modes are activated accordingly to the operating status of the fuel cell, namely starting up, shutting down and normal operation. While the first two modes use heuristic strategies, during normal operation an optimal strategy based on Pontryagin's minimum principle minimizes a cost function that considers the fuel consumption and the deviation from the battery state of charge target. The output of this optimization is then subject to transient and power limitations to extend the system lifetime. In (Fletcher 2016), stochastic dynamic programming is used to produce an optimal strategy for a low speed campus FCEV with the goal of minimizing its fuel consumption and system degradation. The total cost, object of the optimization, includes the degradation of the fuel cell as function of the power, the power change rate and the number of shutting down cycles. The work quantitively considers the effect of the EMS on the voltage degradation of the fuel cell and it gives an estimation of the lifetime increment with respect to an EMS that only considers the fuel consumption minimization. In (Li 2019) an adaptive EMS based on Pontryagin's minimum principle is proposed to minimize the fuel consumption and the power change rate over a receding horizon in which the vehicle speed is predicted through a Markov based velocity predictor. After calculating the future speed sequence, the co-state value is found iteratively until the state of charge at the end of the predictive horizon converges to a reference value. In this case, attention must be paid to the horizon length: for small horizons the EMS will basically work to keep a constant state of charge, penalizing the overall cost function minimization. On the other hand, if the horizon is too long, the speed prediction will be poor and will penalize the EMS performance as well. Other works (Ahmadi 2018, Fu 2019) focus on the EMS of more advanced FCEV powertrain configurations, which include ultracapacitors to absorb dynamic loads and make the FCS and the battery system work in a more stationary way.

In this paper, a standard MPC formulation based on the instantaneous linearization of the powertrain model is used for the online energy management of a heavy-duty fuel cell electric vehicle powered by a PEMFC system and battery system. This control scheme represents a concrete and appealing idea for the online energy management of FCEVs because its theory is mature and has been widely applied in process and chemical industries. The EMS aims to optimize the fuel consumption and the system lifetime through the stationary operation of the FCS. Conversely, the battery system absorbs dynamic loads and its degradation is limited by avoiding excessive discharging and charging, as well as excessive discharging and charging rates. The paper is structured as follows: Section 2 focuses on the modelling of the fuel cell electric vehicle; Section 3 describes the energy management strategies; Section 4 analyses and compares the results obtained through the proposed MPC for a real-world driving mission with those obtained through an offline optimization based on Pontryagin's minimum principle.

2. FUEL CELL ELECTRIC VEHICLE MODELLING

The vehicle model is backward facing, meaning that the power at wheels is calculated from the reference speed profile and then propagates back as electrical power request to the fuel cell system and the battery system. The vehicle is subject to the simple and well-known longitudinal dynamics model (1), where P_w is the power at wheels, m_v is the vehicle mass, v is the vehicle speed, and F_{res} is the overall resistant force opposing to the vehicle.

$$P_w = (m_v \cdot \dot{v} + F_{res}) \cdot v \quad (1)$$

The resistant force considers the aerodynamic drag, the road slope and the wheels rolling friction as in (2), where A_v is the vehicle frontal area, c_x is the drag coefficient, ρ_{air} is the air density, g is the gravitational acceleration, c_r is the rolling friction coefficient and α is the road slope. The vehicle dynamics parameters values are listed in Table 1.

$$F_{res} = 0.5\, A_v\, c_x\, \rho_{air}\, v^2 + m_v\, g(\sin\alpha + c_r \cos\alpha) \quad (2)$$

Table 1. Vehicle Dynamics Parameters

m_v	A_v	c_x	ρ_{air}	c_r
40000 kg	8.0 m^2	0.35	1.2 kg/m^3	0.01

The electric motor is a reversible machine able to convert electrical power into mechanical power to drive the vehicle or to generate electrical power absorbing mechanical power to slow down the vehicle (regenerative braking). The electric motor efficiency depends on the motor torque and speed and on the operation mode (motor or generator). Electric vehicles mostly use permanent magnet synchronous motors because of their high efficiency and specific power. These motors require DC-AC converters (inverters), which determine power losses. Additional power losses are due to drivetrain components, such as gearbox, differential, etc. An exact modelling of all these power losses is not relevant for the purposes of this work, where a constant and total efficiency, η_T, is considered to calculate the electrical power required to drive the vehicle. Auxiliary loads P_{aux} – external to the powertrain – are considered for the calculation of the overall electrical power demand P_{el}, as in (3). These loads are particularly relevant for heavy-duty vehicles (e.g.: cooling trucks), but also for passenger vehicles in specific conditions, e.g. air conditioning power during urban driving. The auxiliary load is considered constant throughout the driving cycle and its value is listed in Table 2, alongside the total efficiency.

$$P_{el} = P_{aux} + P_w \cdot \eta_T^{-\mathrm{sgn}\,(P_w)} \quad (3)$$

2.1 Fuel Cell System

The fuel cell system includes a PEMFC stack and auxiliary components, such as air compressor, humidifiers, hydrogen recirculation pump, cooling pumps. The auxiliary components absorb a considerable amount of power but are indispensable for the stack operation. Therefore, the FCS net power is the stack power subtracted of the auxiliary power: $P_{fcs} = P_{stack} - P_{fc,aux}$. The hydrogen consumption rate W_{H2} is calculated as in

(4), where LHV_{H2} is the hydrogen lower heating value (120 MJ/kg or 33.3 kWh/kg) and η_{fcs} is the fuel cell system efficiency. A quasi-static model of the FCS is considered, neglecting the system response time. Hence, the system efficiency only depends on the FCS power, as shown in Fig. 1.

$$W_{H_2}(P_{fcs}) = \frac{P_{fcs}}{\eta_{fcs}(P_{fcs}) \cdot LHV_{H_2}} \quad (4)$$

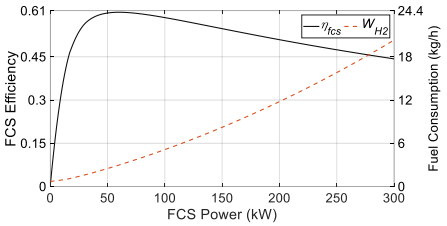

Fig. 1. Fuel cell system efficiency and fuel consumption.

2.2 Battery System

The battery is modelled through a simple equivalent circuit consisting of an ideal voltage source V_{oc} connected in series with a resistor, representing the battery internal resistance R_{int}. The battery terminal voltage V_b is calculated applying Kirchhoff's law (5), assuming the battery current I_b positive in discharging operation.

$$V_b = V_{oc} - R_{int} \cdot I_b \quad (5)$$

The battery open circuit voltage and internal resistance depend on the battery state of charge *SoC*, that is defined in (6) as the ratio between the actual charge *Q(t)* and the nominal charge (or capacity) Q_{nom}. However, these parameters are considered constant for the sake of simplicity and their values are listed in Table 2.

$$SoC(t) = Q(t)/Q_{nom} \quad (6)$$

The battery charge increases if the current is negative (charging operation) or decreases is it is positive (discharging operation), accordingly to (7).

$$\dot{SoC}(t) = -I_b(t)/Q_{nom} \quad (7)$$

The power output of the battery is calculated as the product between the terminal voltage and the current: $P_b = V_b I_b$. Using (5), the battery current can be expressed as a function of the power. Hence, the battery state of charge rate (7) can be expressed as in (8).

$$\dot{SoC}(P_b) = -\left(V_{oc} - \sqrt{V_{oc}^2 - 4 P_b R_{int}}\right)/(2 R_{int} Q_{nom}) \quad (8)$$

2.3 System Constraints

The FCS establishes idling operation at 10% of its nominal power to avoid shut-down cycles. Hence, the FCS power must not exceed its lower and upper limits (9a), $P_{fcs,min}$ and $P_{fcs,max}$ respectively. Similarly, the operation of the battery system is restricted to mitigate degradation phenomena. The state of charge is physically constrained between 0 and 1, but it should also stay – when possible – within assigned lower and upper limits, SoC_{min} and SoC_{max}, to avoid excessive depleting and overcharging (9b). The battery voltage or current are usually constrained to limit the charging and discharging rates, resulting in power lower and upper limits (9c), $P_{b,min}$ and $P_{b,max}$ respectively. All constraint values are listed in Table 2.

$$P_{fcs,min} \leq P_{fcs} \leq P_{fcs,max} \quad (9a)$$

$$SoC_{min} \leq SoC \leq SoC_{max} \quad (9b)$$

$$P_{b,min} \leq P_b \leq P_{b,max} \quad (9c)$$

Table 2. Powertrain Parameters

Parameter	Value		
P_{aux}	10 kW	$P_{fcs,min}$	30 kW
η_T	0.80	$P_{fcs,max}$	300 kW
V_{oc}	380 V	$P_{b,min}$	-150 kW
R_{int}	0.05 Ω	$P_{b,max}$	300 kW
Q_{nom}	200 Ah	SoC_{min}	0.1
		SoC_{max}	0.9

2.4 Real-World Driving Cycle

This work considers a real-world driving cycle obtained from logged data of a conventional heavy-duty commercial vehicle with a sampling time of 1 s. Figure 2 shows the vehicle speed, the road elevation and the electrical power demand, calculated accordingly to (1), (2) and (3). The speed profile is typical of road freight vehicles: frequent acceleration and deceleration phases in urban roads and cruising phases in motorways. Additionally, during the mission, the vehicle enters an urban area for some unloading/loading operations and then it goes back to the motorway. Unlike many other works, the elevation gradient is not neglected, because it highly affects the electrical power demand of heavy-duty vehicles. On steep roads, indeed, the battery operates continuously determining significant energy recuperation (in downhill) or depletion (in uphill) .

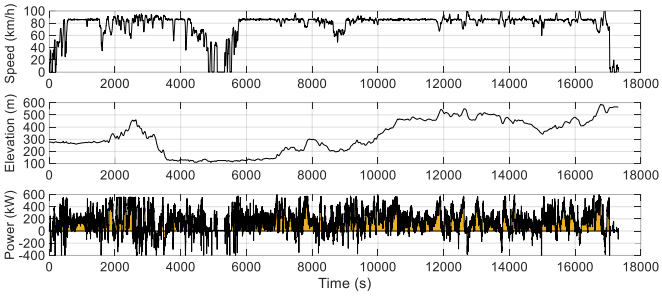

Fig. 2. Driving Cycle: Speed (top), Elevation (middle) and Electrical Power Demand (bottom).

Further details about the driving cycle, the route and the commercial vehicle are not provided because are both confidential and not relevant. Interesting information about the driving cycle are provided in Table 3, where the available regenerative braking energy was calculated considering the battery charging power constraint as well as the FCS idling. One could preliminarily estimate the fuel required to complete the driving mission though (4), assuming a 55% average efficiency: m_{H2} = (833-50)/0.55/33.33 = 42.8 kg.

Table 3. Driving Cycle Characteristics

Driving Time	289 min
Total Distance	372 km
Average Speed	77 km/h
Average Tractive Power	132 kW
Tractive El. Energy Demand	833 kWh
Braking El. Energy Demand	-76 kWh
Available Reg. Braking Energy	-50 kWh

3. ENERGY MANAGEMENT STRATEGIES

Conventional vehicles have zero degrees of freedom on the power distribution since all the load is demanded to the internal combustion engine. Conversely, hybrid vehicles can optimally distribute the load between the power sources to improve performances. In FCEVs, the electrical power demand is provided in combination or solely by the FCS and the battery system (10).

$$P_{el} = P_{fcs} + P_b \tag{10}$$

The control task of optimal power split is referred to as supervisory control or energy management. Heuristic strategies realize the power split following either static maps or set of rules (rule-based) that have been determined beforehand. Optimal strategies find solutions to the control problem with methods from the optimal control theory, minimizing a suitable performance index, usually defined as:

$$J = \int_{T_s} L(\boldsymbol{x}(t), \boldsymbol{u}(t), t)\, dt \tag{11}$$

where L is the instantaneous cost function, x the state variables, u the control variables, and T_s the simulation time span. Many optimization methods have been studied and are available in literature for the energy management of HEVs. Although the overall control problem is different, the optimization methods are suitable for the energy management of FCEVs as well. Dynamic Programming (DP) enables to find the global optimal solution to the control problem. Thanks to this feature and to its capability to handle multiple constraints, DP has been used widely despite its significant computational complexity. Pontryagin's Minimum Principle (PMP) minimizes (11) through the instantaneous minimization of the Hamiltonian of the cost function L. In general, both DP and PMP are offline optimization methods because they require the complete knowledge of the driving mission, but they can also be applied online using predicted future driving conditions. Even though PMP does not guarantee that its solution is the global optimal one, it is more appealing than DP thanks to its lower complexity and because it can be easily extended to online applications. Indeed, the so-called equivalent consumption minimization strategy (ECMS) is an online optimization method deriving from PMP. ECMSs are prominent for energy management applications because they provide near optimal results, only requiring present and past driving information. Conversely, in the model predictive control (MPC) framework future driving conditions are predicted over a finite time horizon. Then, an optimization method is used to find the optimal control law, which is applied for a shorter horizon. The following sections provide a detailed description of the control techniques investigated in this work, i.e. PMP and MPC.

3.1 Pontryagin's Minimum Principle

A control law that satisfies the Pontryagin's minimum principle, i.e. a set of necessary optimality conditions, is called extremal. In general, even though the optimal solution to the control problem is extremal, not all extremal controls are optimal. Hence, the application of the PMP (12) leads to a control law, which may not be the optimal one. However, for many hybrid vehicles energy management applications, the results obtained through the application of the PMP have proven to be optimal and equivalent to those obtained with DP (Serrao 2011). At each time instant t, the extremal control u^* is the one that minimizes the Hamiltonian H of the cost function L, as in (12a) and (12b). The state x and co-state λ evolve according to (12c) and (12d), respectively.

$$H(x(t), u(t), \lambda(t), t) = L(x(t), u(t), t) + \\ + \lambda(t) \cdot \dot{x}(x(t), u(t), t) \tag{12a}$$

$$u^*(t) = \underset{u(t)}{\operatorname{argmin}}\ H(x(t), u(t), \lambda(t), t) \tag{12b}$$

$$\dot{x}(t) = \frac{\partial H}{\partial \lambda}\Big|_{u^*(t)} \tag{12c}$$

$$\dot{\lambda}(t) = -\frac{\partial H}{\partial x}\Big|_{u^*(t)} \tag{12d}$$

In the FCEV energy management problem, there is only one state variable, the battery *SoC*, and one control variable, P_{fcs}. The Hamiltonian is defined as in (13a), setting $L = W_{H2}$ in order to find the absolute minimum fuel consumption of the vehicle. The control $P_{fcs,opt}$ that minimizes the Hamiltonian depends on the electrical power demand and the co-state (13b) as shown in Fig. 3. This optimal control is found numerically accordingly to the power constraints described in (9a) and (9c).

$$H(P_{fcs}, \lambda, P_{el}) = W_{H_2}(P_{fcs}) + \lambda \cdot \dot{SoC}(P_{fcs}, P_{el}) \tag{13a}$$

$$P_{fcs,opt}(\lambda, P_{el}) = \underset{P_{fcs}}{\operatorname{argmin}}\ H(P_{fcs}, \lambda, P_{el}) \tag{13b}$$

$$\dot{SoC}(P_{fcs}, P_{el}) = -\frac{V_{oc} - \sqrt{V_{oc}^2 - 4\,(P_{el} - P_{fcs,opt})\,R_{int}}}{2\,R_{int}\,Q_{nom}} \tag{13c}$$

$$\dot{\lambda} = -\frac{\partial H}{\partial SoC} = 0 \tag{13d}$$

The *SoC* evolves according to (13c), whereas the co-state λ_0 is constant throughout the driving mission because the Hamiltonian does not depend on the state of charge (13d). Here, the co-state assumes the same meaning of the equivalence factor in the ECMS: the battery system is not free to use but comes at a cost, that is the electrical current converted to an equivalent fuel consumption. In Fig. 3, for $\lambda_0 > -2.5$ the FCS exits the idling operation only when the battery system reaches its discharging limit, that is when $P_{el} > 330$ kW. For $\lambda_0 < -8$ and $P_{el} < 150$ kW, the FCS is always working so that the battery system is charged at maximum power, even when the vehicle is in regenerative braking phases.

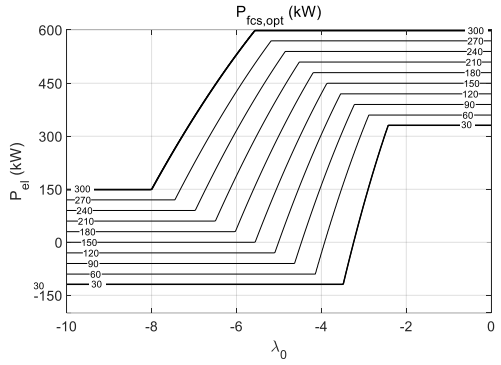

Fig. 3. Optimal FCS Power resulting from the application of the PMP (13). The bold lines mark the maximum power and idle operation of the fuel cell system.

Therefore, a lower magnitude of the co-state determines a higher battery depletion, while a higher magnitude determines a higher battery charging. For each specific driving cycle, the co-state value λ_0 must be found accordingly to the *SoC* target at the end of the driving mission. Usually, this done iteratively (e.g. through the shooting method) until the final *SoC* does not converge to its target.

3.2 Model Predictive Control

Model predictive control (MPC) refers to a wide framework of control strategies that rely on the same principle: optimize the control actions using a model of the system to predict its future outputs over a finite time horizon. In this work, a standard formulation of the MPC based on a discrete linear state-space model is applied to the energy management problem. The augmented state-space model is represented in (14a) and (14b), where $\boldsymbol{x}^k$ are the states at instant *k*, $\boldsymbol{\Delta u}$ and $\boldsymbol{\Delta z}$ are the control and disturbance increments, and *A*, *B*, *C* and *E* are the system matrices. This model predicts the output values $\boldsymbol{Y}$ over the time horizon *h* as in (14c), depending on the set of control actions $\boldsymbol{\Delta U}$ and on the predicted disturbances $\boldsymbol{\Delta Z}$. A standard definition of the matrices *F*, Φ_u and Φ_z can be found in (Wang 2009). The objective function J_h defined in (14d) is minimized to find the optimal set of control actions $\boldsymbol{\Delta U_{opt}}$ as in (14e), where $\boldsymbol{Y_{ref}}$ are the output reference values, *R* and *Q* are semi-positive defined weighting matrices, and $\boldsymbol{\Delta U_c}$ are the feasible controls accordingly to the system constraints.

$$\boldsymbol{x}^{k+1} = A\,\boldsymbol{x}^k + B\,\boldsymbol{\Delta u}^k + E\,\boldsymbol{\Delta z}^k \tag{14a}$$

$$\boldsymbol{y}^k = C\,\boldsymbol{x}^k \tag{14b}$$

$$\boldsymbol{Y} = F\,\boldsymbol{x}^k + \Phi_u\,\boldsymbol{\Delta U} + \Phi_z\,\boldsymbol{\Delta Z} \tag{14c}$$

$$J_h = \left(\boldsymbol{Y_{ref}} - \boldsymbol{Y}\right)^T Q\,\left(\boldsymbol{Y_{ref}} - \boldsymbol{Y}\right) + \boldsymbol{\Delta U}^T R\,\boldsymbol{\Delta U} \tag{14d}$$

$$\boldsymbol{\Delta U_{opt}} = \underset{\boldsymbol{\Delta U}\in\boldsymbol{\Delta U_c}}{argmin}\ J_h \tag{14e}$$

To describe the vehicle model through the discrete linear state-space model, it is necessary to express the state of charge increment ΔSoC as in (15a) and to linearize in each time step its variation with the battery power as in (15b).

$$\Delta SoC(P_b) = \Delta t \cdot \dot{SoC}(P_b) \tag{15a}$$

$$f_\Delta(P_b) = \frac{\partial \Delta SoC}{\partial P_b} = \frac{-\Delta t}{Q_{nom}}\left(V_{oc}^2 - 4\,P_b\,R_{int}\right)^{-1/2} \tag{15b}$$

The system is completely defined by the state space model in (16), where P_b^0 is the battery power used for the linearization in the current operating point. The required electrical power is calculated through (1), (2) and (3), once the future speed has been predicted. However, the speed prediction model is not investigated in this work, and the speed is assumed to be known without uncertainties over the horizon.

$$\boldsymbol{x}^k = \left[SoC^k \quad \Delta SoC^{k-1} \quad P_b^{k-1} \quad P_{fcs}^{k-1}\right]^T; \tag{16}$$

$$\boldsymbol{\Delta u}^k = \left[\Delta P_{fcs}^k\right]; \quad \boldsymbol{\Delta z}^k = \left[\Delta P_{el}^k\right];$$

$$A = \begin{bmatrix}1 & 1 & 0 & 0\\ 0 & 1 & 0 & 0\\ 0 & 0 & 1 & 0\\ 0 & 0 & 0 & 1\end{bmatrix};\ B = \begin{bmatrix}-f_\Delta(P_b^0)\\ -f_\Delta(P_b^0)\\ -1\\ 1\end{bmatrix};\ E = \begin{bmatrix}f_\Delta(P_b^0)\\ f_\Delta(P_b^0)\\ 1\\ 0\end{bmatrix}$$

$$\boldsymbol{y}^k = \left[P_{fcs}^{k-1} \quad SoC^k\right]^T;\ C = \begin{bmatrix}0 & 0 & 0 & 1\\ 1 & 0 & 0 & 0\end{bmatrix};$$

In general, the MPC performs the output reference tracking considering the trade-off with the control effort, minimizing the objective function (14d). However, in the energy management problem, the reference tracking is transformed in a dynamic optimization by writing the objective function as in (17). The cost function (17b) is designed to deviate from the operation at maximum efficiency power $P_{fcs,\eta max}$ only when the battery is depleting/overcharging (first two terms), yet penalizing power change rates (third term). The weights (17c) and (17e) normalize the power terms with respect to their maximum, whereas the weight Q^*_{SoC} goes linearly to zero when the *SoC* approaches its reference value ($SoC_{ref} = 0.75$).

$$J_h = \sum_{k=1}^{h} L^k \tag{17a}$$

$$L^k = Q_P\left(P_{fcs}^k - P_{fcs,\eta_{max}}\right)^2 + \\ + Q^*_{SoC}\left(SoC^{k+1} - SoC_{ref}\right)^2 + Q^*_{\Delta P}\left(\Delta P_{fcs}^k\right)^2 \tag{17b}$$

$$Q_P = 1/P_{fcs,max}^2 \tag{17c}$$

$$Q^*_{SoC}(SoC) = f_1(SoC)\cdot Q_{SoC} \tag{17d}$$

$$Q^*_{\Delta P} = Q_{\Delta P}/P_{fcs,max}^2 \tag{17e}$$

Lastly, to avoid high-power operation of the FCS – when it is possible – the effective maximum power constraint $P^*_{fcs,max}$ is limited between 80% and 50%, depending on the *SoC* (18). Functions f_1 and f_2 depend on the *SoC* as depicted in Fig.4.

$$P^*_{fcs,max}(SoC) = \max\left(f_2(SoC)\cdot P_{fcs,max};\ P_{el} - P_{b,max}\right) \tag{18}$$

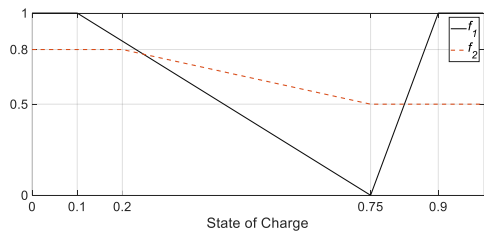

Fig. 4. Functions f_1 and f_2 dependency on the state of charge.

4. SIMULATION RESULTS

The results obtained through the MPC to optimize the fuel consumption and the system lifetime are compared to those corresponding to the absolute minimum fuel consumption, obtained through the PMP. Figure 5 shows *SoC* trajectory, as well as the power and power change rate density distributions. For the considered driving cycle, the FCS operates with a power change rate density distribution significantly narrower around zero than the one corresponding to the PMP optimization. The *SoCs* at the end of the mission are the same in both cases to ensure a meaningful comparison. Figure 6 shows a section of the power split resulting from the MPC and a comparison of the different control laws. Quantitative results are reported in Table 4: thanks to the MPC, the mean absolute power change rate ΔP_{fcs} experiences a 63% reduction and only a 1.5% fuel consumption increment with respect to the absolute minimum, $\Delta m_{H2,PMP}$. This small deviation from the fuel consumption optimality is remarkable considering that the MPC is an online optimization, whereas the PMP is offline and requires the complete knowledge of the driving cycle.

Table 4. Simulation Results: Q_{SoC} = 1e5; $Q_{\Delta P}$ = 2e4.

	PMP	MPC (h = 10 s)	MPC (h = 5 s)
m_{H2}	46.3 kg	47.0 kg	46.9 kg
$\Delta m_{H2,PMP}$	0 %	1.5 %	2.1 %
$mean\|\Delta P_{fcs}\|$	10.4 kW/s	3.8 kW/s	3.9 kW/s
$SoC_{end/max/min}$	0.44/0.81/0.30	0.44/0.66/0.22	0.37/0.56/0.13

The final *SoC* value is close to the initial one (SoC_{start} = 0.5), ensuring the battery charge sustaining. Additionally, the MPC was able to solve the energy management problem even when SoC_{start} was set to SoC_{min}, proving the robustness of the developed energy management strategy. Table 4 also contains the results of an MPC that uses a shorter predictive horizon, showing a slightly higher deviation from the fuel consumption optimality (i.e. 2.1%).

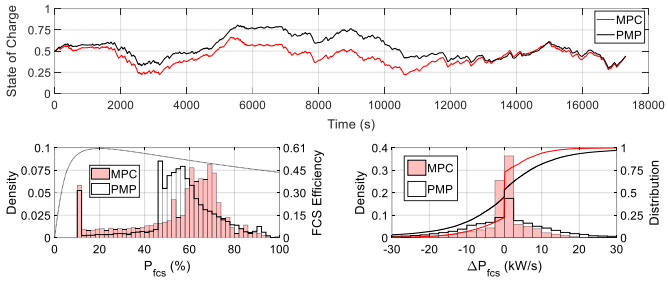

Fig. 5. Comparison of PMP and MPC (h = 10 s) results: State of charge (top); FCS operation density (bottom left); FCS power change rate density and distribution (bottom right).

5. CONCLUSIONS

Thanks to the proposed MPC formulation, the fuel cell lifetime can be extended by achieving a more stationary operation and avoiding shut-down cycles and high-power operations. Remarkably, the fuel consumption is only 1.5% higher than the absolute minimum, which is computed offline. However, it is fundamental to introduce a speed prediction model and to consider additional real-world driving cycles before endorsing the MPC as ideal candidate for the online energy management of heavy-duty FCEVs.

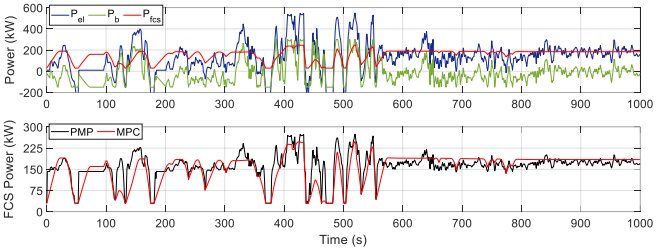

Fig. 6. MPC (h = 10 s) power split (top) and fuel cell power comparison (bottom) with PMP in the first 1000 seconds.

ACKNOLEDGEMENTS

The financial support by the Austrian Federal Ministry for Digital and Economic Affairs and the National Foundation for Research, Technology and Development is gratefully acknowledged. This work has been created in cooperation with the Austrian research project “HyTruck” (grant no. 868790).

REFERENCES

Ahmadi, S., Bathaee, S.M.T., and Hosseinpour, A.H. (2018). Improving fuel economy and performance of a fuel-cell hybrid electric vehicle (fuel-cell, battery, and ultra-capacitor) using optimized energy management strategy. Energy Conversion and Management, vol. 160, pp 74-84.

Borup, R., Meyers, J., Pivovar, B., et al (2007). Scientific Aspects of Polymer Electrolyte Fuel Cell Durability and Degradation. *Chemical Reviews,* vol. 107, pp 3904-3951.

Fletcher, T., Thring, R., and Watkinson, M. (2016). An Energy Management Strategy to concurrently optimise fuel consumption & PEM fuel cell lifetime in a hybrid vehicle. *International Journal of Hydrogen Energy,* volume 41, pp 21503-21515.

Fu, Z., Li, Z., Si, P., and Tao, F. (2019). A hierarchical energy management strategy for fuel cell/battery/supercapacitor hybrid electric vehicles. *International Journal of Hydrogen Energy,* volume 44, 22146-22159.

Li, X., Wang, Y., Yang, D., and Chen, Z. (2019). Adaptive energy management strategy for fuel cell/battery hybrid vehicles using Pontryagin’s Minimal Principle. *Journal of Power Sources,* volume 440, 227105.

Perry, M.L., Patterson, T.W., and Reiser, C. (2006). Systems Strategies to Mitigate Carbon Corrosion in Fuel Cells. *ECS Transactions,* volume 3 (1), pp 783-795.

Serrao, L., Onori, S., and Rizzoni, G. (2011). A Comparative Analysis of Energy Management Strategies for Hybrid Electric Vehicles. *Journal of Dynamic Systems, Measurement, and Control,* volume 133(3), 031012.

Wang, L. (2009). *Model Predictive Control System Design and Implementation Using MATLAB*. Springer.

Xu, L., Li, J., Ouyang, M., et al (2014). Multi-mode control strategy for fuel cell electric vehicles regarding fuel economy and durability. *International Journal of Hydrogen Energy,* volume 39, pp 2374-2389.

Zhao, J. and Li, X. (2019). A review of polymer electrolyte membrane fuel cell durability for vehicular applications: Degradation modes and experimental techniques. *Energy Conversion and Management,* volume 199, 112022.